A.4 Elements of collision theory

The behavior of a many body system depends crucially on the interactions between particles, as epitomized by the BEC-BCS crossover. In the appendix, we review the main tools used to model a two-body elastic interaction.

The study of the interacting and scattering properties of a system is a wide field and can easily be the object of a dedicated work. The objective of this presentation is simply to explicit, without demonstration, most of the concepts used in the previous chapters (scattering length, Feshbach resonance...) and to introduced the tools required to describe interactions in mixed dimensions (chapter 6).

The approach follows essentially that of [Walraven 2010] and [Cohen-Tannoudji and Guery Odelin 2011] to which we refer for all demonstrations of the results stated here.

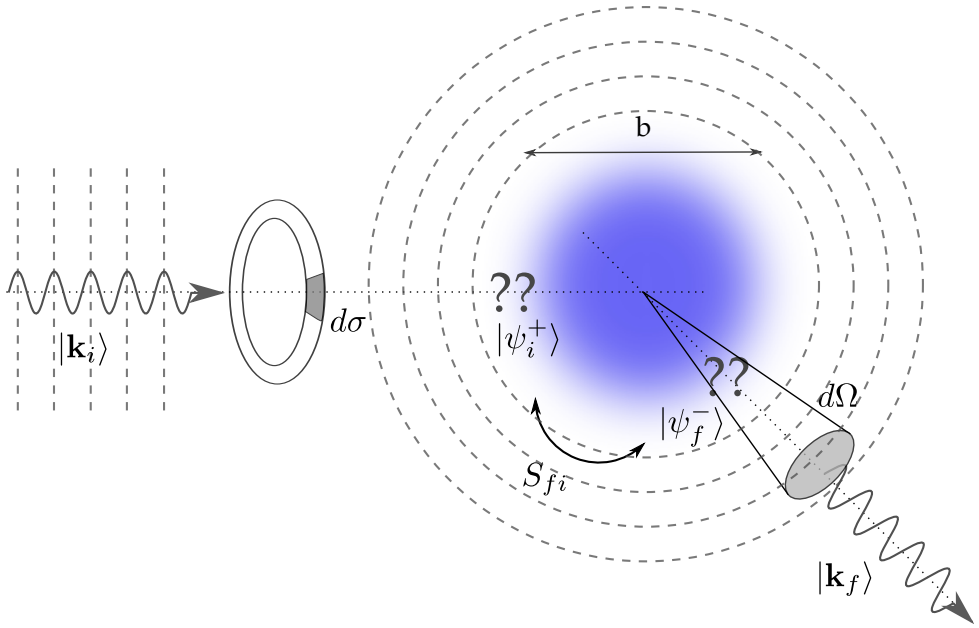

Figure A.5: Scattering on a central potential. An incoming plane wave $|\mathbf{k_i}\rangle$ propagates towards a scattering center of finite range b. Following adiabatically the potential, the initial state becomes $|\psi_i^+\rangle$ close to the center.. The interaction can project the incoming state onto the outgoing state $|\psi_f^-\rangle$, which will in turn become a plane wave $|\mathbf{k_f}\rangle$ far from the center. The probability amplitude of such a scattering is given by the S-matrix element S_{fi}, which can be estimated thanks' to the T matrix. The superposition of all outgoing waves can be described as a spherical wave with the scattering amplitude f. The cross section $d\sigma(\Omega)$ expresses the size of the effective target that leads to a deviation Ω.

A.4.1 Mathematical framework

Let us consider two particles traveling towards each other from a far distance (ie larger than the interaction range). As they move closer, the interaction disturbs their trajectories. Because of energy and momentum conservation, in absence of internal state modification, the particles will eventually separate from each other and resume their motion. The interaction dictates the deviation of the particles or, equivalently, the dephasing of the wavefunction. Those main ingredients are depicted on figure A.5.

We describe the two interacting particles by the wavefunction Ψ and the following Hamiltonian:

$$H_{\text{tot}} = \frac{p_1^2}{2m_1} + \frac{p_2^2}{2m_2} + V(\mathbf{r}_1 - \mathbf{r}_2) \tag{A.46a}$$

$$= \frac{P^2}{2(m_1+m_2)} + \left(\frac{p^2}{2m} + V(\mathbf{r})\right), \tag{A.46b}$$

where we introduced the reduced mass $m = \frac{m_1 m_2}{m_1+m_2}$, the center of mass momentum $\mathbf{P} = \mathbf{p}_1 + \mathbf{p}_2$, the relative momentum $\mathbf{p} = \frac{1}{m}(m_2\mathbf{p}_1 - m_1\mathbf{p}_2)$, and the relative position $\mathbf{r} = \mathbf{r}_1 - \mathbf{r}_2$. Taking advantage of the commutation of the relative- and center-of-mass quantities, we seperate Ψ as

$$\Psi(\mathbf{r}_1, \mathbf{r}_2) = \varphi(\mathbf{R})\,\psi(\mathbf{r}). \tag{A.47}$$

In the following, we will concentrate on the scattering problem described by ψ and the Hamiltonian

$$H = \frac{p^2}{2m} + V(r), \tag{A.48}$$

corresponding to the scattering of a particle on a central potential.

We set the universe in a theorist shoe box of size L, allowing the quantification of wave vectors $|\mathbf{k}\rangle$, eigenstates of $H_0 = p^2/2m$. We also consider an adiabatic switching on and off of the scattering potential overtime, following Gell-Mann and Goldberger:

$$V(\mathbf{r}, t) = V(\mathbf{r}) \exp\left(-\frac{\eta|t|}{\hbar}\right), \tag{A.49}$$

with $\eta \to 0^+$. Qualitatively, this corresponds to considering that the interaction occurs during a finite time. Long before the particle arrives close to the potential center, and long after it was scattered, the interaction is negligible. This allows us to consider quantities long before and long after the scattering:

$$f(\pm\infty) = \lim_{\eta\to 0} \pm \frac{\eta}{\hbar} \int_0^{\pm\infty} f(t) e^{\mp \eta t/\hbar} dt \tag{A.50}$$

A.4.2 Scattering eigenstates

To predict the properties of the interaction, we consider the eigenelements $(\psi_{\mathbf{k}}, E_{\mathbf{k}})$ of the Hamiltonian and review their main properties:

$$H\psi_{\mathbf{k}} = E_{\mathbf{k}}\psi_{\mathbf{k}}. \tag{A.51}$$

- Each state $|\mathbf{k}\rangle$ with energy ϵ_k of the free Hamiltonian H_0 is associated to an advanced and delayed scattering steady state $|\psi^{\pm}_{\mathbf{k}}\rangle$ such that

$$|\psi^{\pm}_{\mathbf{k}}\rangle \equiv U_I\left(0, \mp\infty\right)|\mathbf{k}\rangle \tag{A.52a}$$
$$= \left(1 + G_{\pm}(\epsilon_k)V\right)|\mathbf{k}\rangle \tag{A.52b}$$
$$H|\psi^{\pm}_{\mathbf{k}}\rangle = \epsilon_k|\psi^{\pm}_{\mathbf{k}}\rangle \tag{A.53}$$
$$G_{\pm}(E) = \frac{1}{E - H \pm i\eta} \tag{A.54}$$

  where $U_I(t,t') = \exp\left(-i\frac{t'-t}{\hbar}V\right)$ is the evolution operator in interaction representation. In other words, starting from a plane wave $|\mathbf{k}\rangle$ far from the potential, the wave function becomes $|\psi^{+}_{\mathbf{k}}\rangle$ close to the scattering center but keeps the same energy $\epsilon_{\mathbf{k}}$. Equivalently, a wavefunction $|\psi^{-}_{\mathbf{k}'}\rangle$ close to the scattering center will eventually become a plane wave $|\mathbf{k}'\rangle$ far from it.

- The resolvant $G(E)$ satisfies Dyson equation

$$G(z) = G_0(z) + G_0(z)VG(z), \tag{A.55}$$

  where $G_0(E) = \frac{1}{E - H_0 \pm i\eta}$ is the *resolvent*, whose matrix elements correspond to Green functions. This self consistent equation plays a crucial role to expand perturbatively the scattering elements presented below.

- The scattering eigenstates satisfy Lippman-Schwinger equation

$$|\psi^{\pm}_{\mathbf{k}}\rangle = |\mathbf{k}\rangle + G_{0\pm}(E_k)V|\psi^{\pm}_{\mathbf{k}}\rangle \tag{A.56}$$

A.4.3 Scattering matrices, amplitude and cross section

Because of the scattering, a plane wave $|\mathbf{k}\rangle$ propagating towards the center will give rise to outgoing waves in different directions $|\mathbf{k}'\rangle$ and the properties of the scattering potential dictates the amount radiated in each direction. We introduce the main tools used to describe and predict those deviations.

S Matrix The S matrix characterizes the probability amplitude for an incident state $|\mathbf{k}\rangle$ to

emerge as an outgoing state $|\mathbf{k}'\rangle$ after the collision.

$$S_{\mathbf{k}',\mathbf{k}} = \langle \mathbf{k}' | U_I(-\infty, +\infty) | \mathbf{k} \rangle \tag{A.57a}$$
$$= \langle \psi^-_{\mathbf{k}'} | \psi^+_{\mathbf{k}} \rangle, \tag{A.57b}$$

ie the probability amplitude is the overlap between the initial state forward propagated to the potential and the final state retropropagated to the potential (see figure A.5).

T Matrix

The T matrix is directly related to the S matrix by the relation

$$S_{fi} = \delta_{f,i} - 2i\pi\delta\left(E_f - E_i\right) T_{fi}. \tag{A.58}$$

The point of this relation is that the T matrix can be easily expanded in terms of the interaction potential V and the resolvant G, allowing its evaluation. Using Dyson equation, the T matrix takes the following form

$$T = V + VGV = V + VG_0V + VG_0VG_0V + ... \tag{A.59}$$

Scattering amplitude

Far away from the scattering center, the scattering eigenstates are plane waves. Closer to the center, they can be expressed as the superposition of a plane wave and a spherical wave, which amplitude in the direction $\mathbf{u}$ is given by the scattering amplitude $f(\mathbf{k}, \mathbf{u})$:

$$\psi^+_{\mathbf{k}}(r\mathbf{u}) \simeq \frac{1}{\sqrt{L^3}} e^{i\mathbf{k}.\mathbf{r}} + \frac{1}{\sqrt{L^3}} f(\mathbf{k}, \mathbf{u}) \frac{e^{ikr}}{r} \tag{A.60}$$

where

$$f(\mathbf{k}, \mathbf{u}) = -\frac{m\sqrt{L^3}}{2\pi\hbar^2} \int d^3\mathbf{r}'\, e^{-i\mathbf{k}.\mathbf{r}'} V(\mathbf{r}') \psi^+_{\mathbf{k}}(\mathbf{r}') \tag{A.61}$$

The scattering amplitude is the natural description of the cross section, presented below. It can be estimated from the T matrix through the relation

$$f(k, \mathbf{n}, \mathbf{u}) = -\frac{mL^3}{2\pi\hbar^2} \langle k\mathbf{u}|T|\mathbf{k}\rangle \tag{A.62}$$

Cross sections

The differential cross section $\frac{d\sigma}{d\Omega}$ express the likelihood for an incoming particle to be scattered in the solid angle Ω. More quantitatively, with an incoming particle flux ϕ_i, the outgoing flux ϕ_s at a distance r in the solid angle Ω with a precision $d\Omega$ is set by:

$$\phi_i d\sigma = \phi_s(r, \Omega) r^2 d\Omega. \tag{A.63}$$

Taking into account the symmetry properties of indistinguishable particles, the differential cross section corresponding to the scattering from $\mathbf{k}$ to $\mathbf{k}'$ is related to the scattering amplitude through

$$\frac{d\sigma}{d\Omega}(\mathbf{k}\to\mathbf{k}') = \begin{cases} |f(k,\theta)+f(k,\pi-\theta)|^2 & \text{for bosons} \\ |f(k,\theta)-f(k,\pi-\theta)|^2 & \text{for fermions} \\ |f(k,\theta)|^2 & \text{for distinguishable particles} \end{cases} \tag{A.64}$$

where θ is the angle between $\mathbf{k}$ and $\mathbf{k}'$. The total cross section expresses the likelyhood for a particle to be deviated in any direction. It is related to the scattering amplitude through the *optical theorem*, which expresses the flux conservation

$$\sigma_{\text{tot}}(k) = \int d\Omega\, \frac{d\sigma}{d\Omega} = \frac{4\pi}{k}\text{Im}\left(f\left(k,\theta=0\right)\right). \tag{A.65}$$

A.4.4 Low energy limit

When considering ultracold atoms, further simplifications allow to summarize the effect of the interaction to few scalar parameters, notably the scattering amplitude, which we introduce in this section.

Assuming a spherical interaction potential, we decompose the wavefunction into spherical harmonics with increasing orbital momentum l. Because of energy and momentum conservation, the effect of the scattering is essentially described by the dephasing η_l accumulated be each partial wave during the process. We express the scattering amplitude and cross section as a sum over all spherical modes:

$$f(k,\theta) = \sum_{l=0}^{+\infty}(2l+1)f_l \mathrm{P}_l(\cos(\theta)) \tag{A.66a}$$

$$f_l = \frac{1}{2ik}\left(e^{2i\eta_l(k)}-1\right) \tag{A.66b}$$

$$\sigma_l(k) = 4\pi\sum_l(2l+1)|f_l|^2 \tag{A.67a}$$

$$= \frac{4\pi}{k^2}\sum_l(2l+1)\sin^2\eta_l \tag{A.67b}$$

where P_l are Legendre polynomials and $\eta_l(k)$ is the phase shift of the partial wave l.

For arbitrary potential with a finite range b, this phase can be written in the low energy limit as:

$$\tan\eta_l \underset{kr\to 0}{\simeq} -\frac{2l+1}{\left[(2l+1)!!\right]^2}(ka_l)^{2l+1}, \tag{A.68}$$

where a_l is the l-wave *scattering length*. The result can be extended for power-law potential $V \propto r^{-s}$ for partial waves $l < \frac{1}{2}(s-3)$.

Each spherical harmonic contributing to the wavefunction has a angular momentum $l(l+1)\hbar^2$. At the range of the interaction potential, this momentum results in a kinetic barrier which

can be overcome only if the kinetic energy of the colliding particle is high enough:

$$\frac{\hbar^2 k^2}{2m} > \frac{l(l+1)\hbar^2}{b^2} \Leftrightarrow \frac{2\pi b}{\lambda_{\mathrm{dB}}} > l \tag{A.69}$$

As a result, at low energy $\lambda_{\mathrm{dB}} \gg b$, only the first harmonic $l = 0$, the so-called *s-wave*, will contribute to the scattering.

S wave collisions Considering equation (A.68), we introduce the scattering length a and the effective interaction length r_e to expand the s-wave phase shift:

$$\cot(\eta_0) = -\frac{1}{ka} + \frac{1}{2} k r_e + ... \tag{A.70}$$

The scattering amplitude and the cross section for distinguishable particles thus take the form

$$f_0 = \frac{1}{k\cot(\eta_0) - ik} \simeq \frac{1}{-\frac{1}{a} + \frac{1}{2} r_e k^2 - ik} \tag{A.71a}$$

$$\sigma_0(k) = 4\pi |f_0|^2 = \frac{4\pi a^2}{\left(1 - \frac{1}{2} a r_e k^2\right) + (ka)^2} \tag{A.71b}$$

If the interaction can be reduced to the single *s-wave* contribution, it is entirely described at low energy by the scattering length, which accounts for the dephasing induced by the collision. The specificities of the potential can then be neglected and the scattering is equivalent to the one caused by a pseudo potential:

$$U(\mathbf{r}) = \frac{2\pi\hbar^2}{m} a \times \delta(\mathbf{r}) \frac{\partial}{\partial r} r. \tag{A.72}$$

Singlet and triplet scattering length To describe the interaction between two alkali atoms, the spin degree of freedom must also be taken into account. Considering only the electrons, the spin configuration can be either symmetric (triplet state) or anti-symmetric (singlet). Because of Pauli principle, the symmetry will constrain the orbital wave-function of the electron cloud and thus the interaction experienced by the atoms at a given internucleus distance r. The interatomic electrostatic potential should therefore be expressed as the superposition of a singlet and triplet potential:

$$V_{\mathrm{el}}(\mathbf{r}) = V_{\mathrm{s}}(\mathbf{r}) \left|S = 0\right\rangle \left\langle S = 0\right| + V_{\mathrm{t}}(\mathbf{r}) \left|S = 1\right\rangle \left\langle S = 1\right| \tag{A.73}$$

$$= V_D(\mathbf{r}) + J(\mathbf{r})\, \mathbf{S_1}.\mathbf{S_2}, \tag{A.74}$$

where $\mathbf{S} = \mathbf{S}_1 + \mathbf{S}_2$ is the total electronic spin, $V_{\mathrm{D}} = \frac{1}{4}\left(V_{\mathrm{s}} + 3V_{\mathrm{t}}\right)$ and $J = V_{\mathrm{t}} - V_{\mathrm{s}}$. At low temperature, the singlet and triplet potential result in scattering lengths a_s and a_t respectively. The triplet scattering length notably accounts for the collisions

	^{6}Li-^{6}Li	^{6}Li-^{40}K	^{40}K-^{40}K
a_s/a_0	39	52	104
a_t/a_0	-2200	63	169
Ref.	[Ottenstein *et al.* 2008]	[Falke *et al.* 2008]	[Wille *et al.* 2008]

Table A.3: singlet and triplet scattering length for the atoms at stake in the FERMIX experiment. The values are expressed in units of Bohr radius $a_0 = 52.92$ pm.

between stretch-states. Their values for Li and K are given in table A.3

P wave collisions For spin polarized fermions, the symmetry of the internal state forbids any symmetric external wave-function because of Pauli principle. S-wave collisions are thus ruled out and the first contributing order is given the so called *p-wave* collisions,

$$\cot(\eta_1) = -\frac{3}{k^3 a_1^3} + \frac{1}{k r_1}. \tag{A.75}$$

The scattering amplitude and the cross section for distinguishable particles take the form

$$f_1 = \frac{1}{k\cot(\eta_1) - ik} \simeq \frac{1}{-\frac{3}{k^2 a_1^3} + \frac{1}{r_1} - ik^2} \tag{A.76a}$$

$$\sigma_1(k) = 12\pi |f_1|^2 = \frac{12\pi a_1^2}{\left(\frac{a_1}{r_1} - \frac{3}{k^2 a_1}\right)^2 + a_1^2 k^2} \tag{A.76b}$$

Note that the first spherical harmonic is anti-symmetric and p-wave collisions are therefore forbidden for indistinguishable bosons.

Temperature dependence The cross section of s- and p-waves collisions at finite temperature can be estimated as

$$\sigma_{s,p}(T) = \int d^3\mathbf{k}\, n(\mathbf{k}, T)\sigma_{s,p}(\mathbf{k}) \tag{A.77}$$

where $n(\mathbf{k}, T)$ is the density of particles in momentum space at temperature T. For distinguishable particles, p-waves predominate at high temperatures but vanish at low temperature. The crossover regime is around 6 mK for Lithium. For Potassium, p waves collisions predominates over s-waves until $\sim 100\,\mu$K and remain significant until $20\,\mu$K [DeMarco *et al.* 1999].

A.4.5 Feshbach resonances

Initially introduced in nuclear physics [Feshbach 1962], Feshbach resonances are the experimental way to tune the interactions at will; they are one of those magical knobs that make

cold atoms such a versatile platform. Here, we simply introduce the main concepts behind scattering resonances. For a detailed review, see [Chin *et al.* 2010].

Because of energy and momentum conservation, two elastically interacting particles cannot form a bound state and will eventually leave as free states. Nevertheless, the existence of bound states can strongly alter the scattering properties as a virtual coupling between the open and closed channel will change phase shifts. This coupling is that much stronger as the energy of both state are equal, just like the scattering of light by a two levels system is maximal as the light has the same frequency as the atomic transition. Close to resonance, the energy difference between bound and scattering states dictates the value of the scattering length; if this difference can be adjusted, any scattering length can be achieved.

More quantitatively, considering a zero energy scattering state $|\psi_0^+\rangle$ coupled by the Hamiltonian W to a bound state $|\psi_{\text{res}}\rangle$ of energy E_{res} close to 0 (see figure A.6), the scattering length takes the form:

$$a = a_{\text{bg}} + \frac{2\pi^2 m}{\hbar^2} \frac{\left|\langle \psi_0^+ | W | \psi_{\text{res}} \rangle\right|^2}{E_{\text{res}} + \Delta E}, \tag{A.78}$$

where the background value a_{bg} is the scattering length in absence of coupling and ΔE is the energy shift of the bound state induced by the coupling.

Experimentally, the most usual way to take advantage of this effect is the so-called *magnetic Feshbach resonance*, which plays on the differential Zeeman shift between the singlet and triplet states. Because they don't have the same magnetic moment, the singlet and triplet states don't experience the same energy shift in a given magnetic field. At low energy, only the lowest state is accessible and provides scattering states $|\psi_0^+\rangle$ (open channel). However, the magnetic interaction between electronic spins can couple both states and transfer colliding atoms to a bound state $|\psi_{\text{res}}\rangle$ with an energy close to the scattering state (closed channel). By tuning on the magnetic field, it is possible to adjust the energy difference between $|\psi_0^+\rangle$ and $|\psi_{\text{res}}\rangle$, leading to a divergence of the scattering length when the two energies coincides. Close to the resonance, the scattering length takes indeed the form [Moerdijk *et al.* 1995]:

$$a = a_{\text{bg}} \left(1 - \frac{\Delta B}{B - B_0}\right), \tag{A.79}$$

where B is the applied magnetic bias, B_0 is the field for which both states have the same energy (including the energy shift due to the coupling) and ΔB is the width of the resonance.

In addition to the elastic process considered in this section, inelastic collisions resulting in atom losses are also increased close to Feshbach resonances and should be taken into account in a more quantitative approach.

The idea of tuning cold atoms interaction through magnetic Feshbach resonances was proposed in the early '90s [Tiesinga *et al.* 1993] and realized soon after [Inouye *et al.* 1998]. The same strategy can be applied with other means to control the energy difference between a

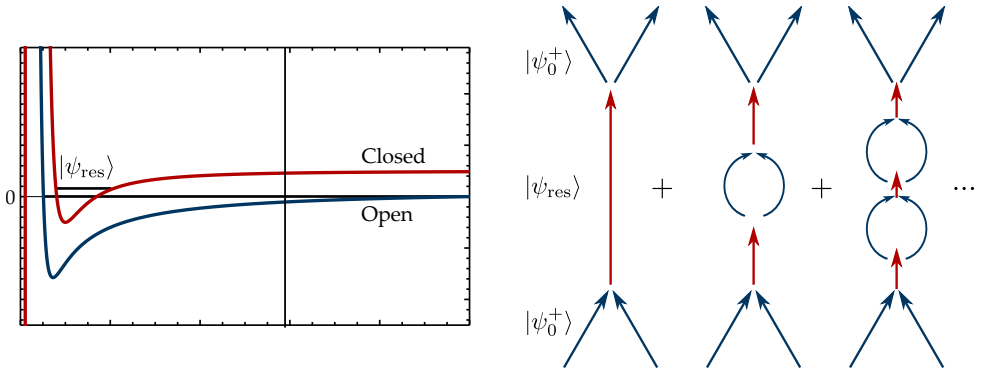

Figure A.6: Feshbach resonance. **Left**: Two channel model. At finite magnetic field, the singlet state (red) is up shifted with respect to the triplet state (blue), which is therefore the only accessible channel (open channel) for scattering states with lowest energy $|\psi_0^+\rangle$. The energy difference between the closed channel bound state $|\psi_{\rm res}\rangle$ and the scattering state $|\psi_0^+\rangle$ determine the value of the scattering length. **Right**: Resonant scattering. Just like the scattering of light by a two level system, the elastic interaction of two atoms is strongly altered when bound and scattering states have equal energy, allowing an efficient virtual coupling between both states.

bound state in the closed channel and a scattering state in the open channel, such as microwave [Papoular *et al.* 2010], RF- [Moerdijk *et al.* 1996] or optical [Theis *et al.* 2004] dressing. Those alternatives allow the simultaneous and independent control of several scattering lengths in a multicomponent gas [Zhang *et al.* 2009].

A.4.6 Getting familiar with a Feshbach resonance

As mentioned before, ^{40}K features a 7 G wide Feshbach resonance at 202 G, allowing a complete control over the scattering length between $|-9/2\rangle$ and $|-7/2\rangle$ states. So far, we did not take advantage of this resonance on the FERMIX experiment and several text-book measurements could be useful to develop a better knowledge of our system [Ketterle and Zwierlein 2008]. One easy way to observe a resonance is to measure the reduced lifetime due to the increase of the inelastic scattering rate [Courteille *et al.* 1998]. However, a more accurate study shows that the maximal three body losses enhancement is located well below the actual resonance.

A more accurate method to determine the position of a Feshbach resonance is to study the formation of Feshbach molecules. At large positive scattering length, two colliding atoms described by the two channel Hamiltonian present a bound state of energy:

$$E_b \sim \frac{\hbar^2}{2\mu a^2}, \tag{A.80}$$

where $a > 0$ is the scattering length and μ the reduced mass. Atoms can be adiabatically transfered to this *Feshbach molecule* as they follow the lowest energy state through a sweep across the Feshbach resonance, starting from a small negative scattering length [Regal *et al.* 2003].

Experimentally, this can be done by ramping the magnetic bias; the sweeping time should be slow compared to the Landau-Zener rate $0.11\ \mathrm{G}/\mu\mathrm{s}/10^{13}\ \mathrm{cm}^{-3}$ for ^{40}K, but fast enough to limit enhanced losses induced by the resonance. A transfer efficiency up to 90% can be achieved with this method.

When imaging the cloud at the atomic resonant wavelength λ, molecules are transparent if $a \lesssim \lambda/2\pi$ and the formation of molecules appears as a decrease of the atom number. On the other hand, the total atom number is restored by ramping the field back up to its initial value. At colder temperatures, molecules undergo Bose-Einstein condensation and the distribution presents a characteristic bimodal distribution [Zwierlein *et al.* 2005b].

A radio-frequency radiation with a frequency resonant with the binding energy (A.80) can dissociate the molecules, revealing their presence [Chin *et al.* 2004]. With such a RF-spectroscopy, it is possible to determine the onset of molecular dissociation and hence the value of the field for which (A.80) vanishes [Bartenstein *et al.* 2005]. While this method is particularly well suited for ^{6}Li, for which the electron and nuclear spins are decoupled as soon as the magnetic field exceeds few hundreds of Gauss, rendering the resonant frequency very insensitive to small magnetic fluctuations (1.5 kHz/G for the $|1/2, 1/2\rangle \to |1/2, -1/2\rangle$ transition at 800 G). A satisfying resolution can thus be achieved without dedicated field stabilization. By contrast, for ^{40}K, the resonant frequency of the $|9/2, -9/2\rangle \to |9/2, -7/2\rangle$ transition close to the 202 G Feshbach resonance varies by 150 kHz/G, but this increased sensitivity is still sufficient to allow for measurements with kilohertz resolution.